The 15th International Symposium on Magnetic Bearings, August 3-6, 2016, Mojiko Hotel, Kitakyushu, Japan

ISMB15

Control of a single parallel winding bearing-less machine

Nicolas SCHNEIDER*, Puvan ARUMUGAM***, Herve MORVAN*, Seamus GARVEY** and Tahar HAMITI****

*Institute for Aerospace Technology, Aerospace Technology Centre, The University of Nottingham, Nottingham, UK

**Faculty of Engineering, The University of Nottingham, Nottingham, UK

***Force Engineering, Gelders Hall Road, Shepshed, Leicestershire, LE12 9NH, UK

****VEDECOM, 77 rue des Chantiers, 78000 Versailles, France

E-mail: nicolas.schneider@nottingham.ac.uk

Abstract

This paper proposes a control method for a bearing-less machine (BELM). Unlike most machines that use two separate windings - one for the torque generation and one for the force generation - this study will concentrate on a BELM using a single winding that is able to fulfil the two functions. A model of this BELM was set based on the circuit equation of the electrical machines. Two inductance parameters within the model were introduced to simplify the model of the machine and ease its control. An algebraic formulation of the BELM's forces is found using an analytical model of the flux changes in the coils as a function of the displacement of the rotor. This is used for the formulation of the energy in the airgap. The obtained results using the analytical model are compared and verified via FEM results. Based on the analytical model of the BELM, a control system that includes a switching functionality for the Voltage Source Inverter (VSI) is implemented to investigate the dynamic control behavior. In addition, a sub-model of the rotating shaft is integrated within the dynamic model to introduce the shaft's displacement. The obtained results under healthy and different displacement scenarios demonstrate the validity and the performance of the proposed control method for the BELM.

Keywords : Bearingless Machine, Control, Vibration

1. Introduction

The reduction of vibration using bearing-less machines (BELM) has already been studied on different machine topologies; Induction Machines (IM), Switch Reluctance (SR) machines and Permanent Magnet (PM) machines [1, 2]. In [3, 4], a Middle-Point Current-Injection technique is introduced to suppress the vibration in the single winding BELM topology. However, a vibration suppression method using a single winding BELM has not been extensively investigated. Within this paper an effort is taken to suppress the vibration introduced in such single wining machines. A control method for a BELM, using a single winding which generates the torque as well as the suspension force to restrain the shaft, is introduced. A single topology using two parallel coils for each phases is focused on[5]. Fig. 1 and Fig. 2 show the 2-poles, 12-slots PM machine and the arrangement of the winding considered in the study, respectively. The working principle of the machine can be found in detail in [5, 6]. In order to create a control for the suspension currents, as well as the current associated to the torque generation, at first a model of the BELM is established. An inductance for the suspension system and the torque system are introduced to simplify the model. A relationship between the feed suspension current and the suspension forces is formed through two different force calculation methods. Finally, the methods are verified through Finite Element (FE) analysis. The control system was then evaluated to see its impact on the vibration of the shaft.

2. Model for the Bearingless machine

The proposed model can be categorized into two parts. The first part is to explicit the electrical behavior of the machine using the fundamental voltage equations as given in (1) and (2). From the equation, it can be seen that the two current variables are dependant on, and correlated with, each other. In order to separate the two current variables, an equation related to the voltage of a coil was developed. Since the supply is three phase, and thus the sum of the current is equal to zero under balanced condition, the following assumptions are adopted:

1. The magnetic materials are considered linear
2. The coils are considered perfectly identical
3. The displacement of the rotor are considered small and therefore do not generate any significant change in the coil's inductance.

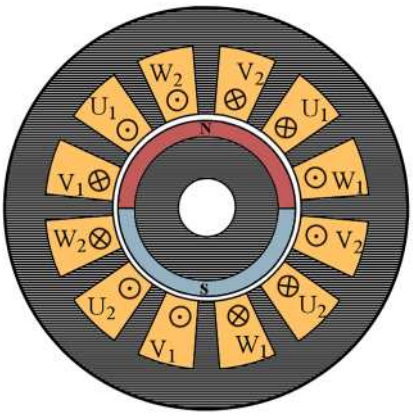

Fig. 1 Bearingless machine topology

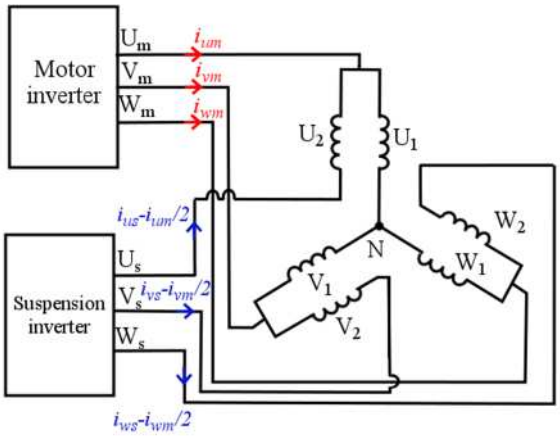

Fig. 2 Winding configuration

$$[V]=[R]\wedge[I]+[L]\wedge\frac{d}{dt}[I]+[E] \tag{1}$$

$$\begin{bmatrix}V_{u1}\\V_{u2}\\V_{v1}\\V_{v2}\\V_{w1}\\V_{w2}\end{bmatrix}=\begin{bmatrix}R&0&0&0&0&0\\0&R&0&0&0&0\\0&0&R&0&0&0\\0&0&0&R&0&0\\0&0&0&0&R&0\\0&0&0&0&0&R\end{bmatrix}\times\begin{bmatrix}\frac{i_{Um}}{2}+i_{Us}\\\frac{i_{Um}}{2}-i_{Us}\\\frac{i_{Vm}}{2}+i_{Vs}\\\frac{i_{Vm}}{2}-i_{Vs}\\\frac{i_{Wm}}{2}+i_{Ws}\\\frac{i_{Wm}}{2}-i_{Ws}\end{bmatrix}+\begin{bmatrix}L&M_1&M_2&M_3&M_2&M_3\\M_1&L&M_3&M_2&M_3&M_2\\M_2&M_3&L&M_1&M_2&M_3\\M_3&M_2&M_1&L&M_3&M_2\\M_2&M_3&M_2&M_3&L&M_1\\M_3&M_2&M_3&M_2&M_1&L\end{bmatrix}\times\frac{d}{dt}\begin{bmatrix}\frac{i_{Um}}{2}+i_{Us}\\\frac{i_{Um}}{2}-i_{Us}\\\frac{i_{Vm}}{2}+i_{Vs}\\\frac{i_{Vm}}{2}-i_{Vs}\\\frac{i_{Wm}}{2}+i_{Ws}\\\frac{i_{Wm}}{2}-i_{Ws}\end{bmatrix}+\begin{bmatrix}E_{u1}\\E_{u2}\\E_{v1}\\E_{v2}\\E_{w1}\\E_{w2}\end{bmatrix} \tag{2}$$

From (2), the voltage equation of a coil can be represented as follows:

$$v_{U1}=R\cdot\left(\frac{i_{Um}}{2}+i_{Us}\right)+\frac{1}{2}\cdot\left(L+M_1-M_2-M_3\right)\cdot\frac{di_{Um}}{dt}+\left(L-M_1-M_2+M_3\right)\cdot\frac{di_{Us}}{dt}+E_{U1} \tag{3}$$

Equation (3) can be simplified as in (4) by denoting two inductance terms L_m and L_s, which represent the inductance of the torque generating part of the machine and the suspension part, respectively

$$v_{U1}=R\cdot\left(\frac{i_{Um}}{2}+i_{Us}\right)+\frac{1}{2}\cdot\left(L_m\right)\cdot\frac{di_{Um}}{dt}+L_{s\cdot}\cdot\frac{di_{Us}}{dt}+E_{U1} \tag{4}$$

The objective being to control this BELM, the voltages on the two converters was calculated using the Eq.(3) and Eq.(4). The voltage, for the torque generating function will be named v_{Um}, v_{Vm}, v_{Wm} and the suspension part named v_{Us}, v_{Vs}, v_{Ws}. Thus, the phase voltage can be re-written as

$$v_{Um}=\frac{1}{2}\cdot\left(R\cdot i_{Um}+L_m\cdot\frac{di_{Um}}{dt}\right)+E_{U1}+\frac{v_{Us}}{2} \tag{5}$$

Where,

$$v_{Us}=2\cdot R\cdot i_{Us}+2\cdot L_s\cdot\frac{di_{Us}}{dt} \tag{6}$$

Eq.(6) show that the voltage of the suspension inverter depends only of the suspension current. Considering that$E_{U1}+\frac{v_{Us}}{2}$ is a perturbation in Eq.(5) the two currents can now be considered decoupled. The two new equations obtained, Eq.(5) Eq.(6), will be the base for the control of the BELM.

3. Force calculation

The control can be effectively implemented if the relationship between the currents applied and the suspension forces is known. The calculation of the forces can be made using different methods; through Spectral analysis of field sources [7], using the electromagnetic energy [8, 9]. In this article the force was calculated using the energy. The energy (W) is estimated and the force f_e and the direction e are predicted. In order to predict the force, a formulation of the inductances depending on the position of the rotor is identified.

In order to obtain the variation of the inductance and flux over the direction of displacement of the rotor, a formulation of the airgap depending on the displacement has been calculated. Where e_o is the airgap of the BELM and $\delta(x_o, y_o, \beta)$ is the displacement of the rotor depending of the angle β and the coordinates of the centre of the rotor x_o and y_o. The used formulation eases the derivations from Eq. (6). Assuming that the inductance of coils is defined by a constant λ over the airgap of the BELM, the Eq. (7) is implemented in the previous definition of the Inductance, where the two angles β_1 and β_2 correspond to the angles of the flux path direction. The formulation is then derivate in a chosen direction. To obtain the expected result the derivation was done on x and y, but for the sake of simplicity only the x direction is shown here. Considering that the sum of the two displacements is relatively small, the equation can be developed in a Taylor series [10]. This enables the development ofa simpler expression for the inductance of the coils. For the flux generated by the magnets, the same approached has been used. Based on the fact that the flux created by the magnet can be defined as in Eq. (11), where l_{mag} is the thickness of the magnets and $\psi(\theta)$ is function depending on the position of the rotor. Using the same process than for the inductance, the flux of the magnets has been simplified to obtain Eq. (12).

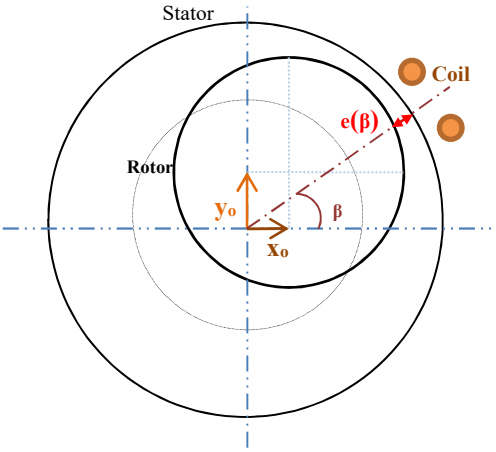

Fig. 3 Airgap formulation schematic

$$W = \frac{1}{2} \cdot [I]^t \wedge [L] \wedge [I] + [I]^t \wedge [\varphi_{mag}] \tag{7}$$

$$f_e = \frac{\partial W}{\partial e} = \frac{1}{2} \cdot [I]^t \wedge \left[\frac{\partial L}{\partial e}\right] \wedge [I] + [I]^t \wedge \left[\frac{\partial \varphi_{mag}}{\partial e}\right] \tag{8}$$

$$e(\beta) = e_o - \delta(x_o, y_o, \beta) \tag{9}$$

$$\delta(x_o, y_o, \beta) = x_o \cdot \cos(\beta) + y_o \cdot \sin(\beta) + \sqrt{\rho - R_{rotor}^{\ 2}}$$
$$\rho = \cos(\beta)^2 \cdot (x_o^{\ 2} - y_o^{\ 2}) + 2 \cdot \sin(\beta) \cdot \cos(\beta) \cdot x_o \cdot y_o - x_o^{\ 2} + R_{rotor}^{\ 2} \tag{10}$$

$$L_o = \frac{\lambda}{2 \cdot e_o} \tag{11}$$

$$L = \frac{\lambda}{2 \cdot e_o - (\delta(x_o, y_o, \beta_1) + \delta(x_o, y_o, \beta_2))} \tag{12}$$

$$L = L_o \cdot \left(1 + \frac{\delta(x_o, y_o, \beta_1) + \delta(x_o, y_o, \beta_2)}{2 \cdot e_o}\right) \tag{13}$$

$$\varphi_o(\theta) = \frac{\psi(\theta)}{1 + \mu_r \dfrac{e_o}{l_{mag}}} \tag{14}$$

$$\varphi(\theta) = \varphi_o(\theta) \cdot \left(1 + \frac{\mu_r \cdot \delta(x_o, y_o, \beta)}{l_{mag} + \mu_r \cdot e_o}\right) \tag{15}$$

The two expressions must be derivate in order to obtain the force generated by the BELM as shown in Eq. (8). To do so, the expression of the displacement $\delta(x_o, y_o, \beta)$ has been derivate in the two directions, x and y. The equations have been explicated only for the x_o direction, as the result was naturally the same in the other direction. The derivation of this displacement presents two parts. The first part depends only on the angle of the coil's direction. The second part depends on the parameter ρ, introduced before Eq.(10), which is a complex composition of the different displacements - x_o and y_o - and the angle β. To simplify the previous equation, Eq.(16), the part depending on ρ was studied separately. Considering that x_o and y_o are very small compared to the other parameters of the equation, the limit of this portion of the equation is equal to 0 Eq.(17). This equation is detailed in the annexes. This leads to a simplification of the expression of the derivation of $\delta(x_o, y_o, \beta)$ in x_o and y_o directions Eq.(18). This result was then applied in order to get the derivative of the inductance matrix and the flux vector.

$$\frac{\partial \delta(x_o, y_o, \beta)}{\partial x_o} = \cos(\beta) + \frac{\dfrac{\partial \rho}{\partial x_o}}{2 \cdot \sqrt{\rho}} \tag{16}$$

$$\lim_{\substack{x_o \to 0 \\ y_o \to 0}} = \frac{\dfrac{\partial \rho}{\partial x_o}}{2 \cdot \sqrt{\rho}} = 0 \tag{17}$$

$$\begin{cases} \dfrac{\partial \delta(x_o, y_o, \beta)}{\partial x_o} = \cos(\beta) \\ \dfrac{\partial \delta(x_o, y_o, \beta)}{\partial y_o} = \sin(\beta) \end{cases} \tag{18}$$

$$\begin{cases} \dfrac{\partial L}{\partial x_o} = \dfrac{L_o}{2 \cdot e_o} \cdot (\cos(\beta_1) + \cos(\beta_2)) \\ \dfrac{\partial L}{\partial y_o} = \dfrac{L_o}{2 \cdot e_o} \cdot (\sin(\beta_1) + \sin(\beta_2)) \end{cases} \tag{19}$$

$$\begin{cases} \dfrac{\partial \varphi(\theta)}{\partial x_o} = \varphi_o(\theta) \cdot \dfrac{\mu_r \cdot \cos(\beta)}{l_{mag} + \mu_r \cdot e_o} \\ \dfrac{\partial \varphi(\theta)}{\partial y_o} = \varphi_o(\theta) \cdot \dfrac{\mu_r \cdot \sin(\beta)}{l_{mag} + \mu_r \cdot e_o} \end{cases} \tag{20}$$

The results obtained in the Eq. (19) to (20) are then integrated in the Eq. (8) to obtain the force generated by the BELM. To validate the results of this equation, they are compared to an FEM calculation. The **Error! Reference source not found.**shows that for a defined current, the forces calculated using the energy and the FEM are similar and only present a difference of about 5%. The difference that remains could be explained by the fact that the algebraic formulation does not take in account the non-linearity of the materials and an Iron with an infinite permeability. Further development should be done in the future to reduce even the gap.

It must be noted that the force generated by the inductance matrix of the BELM is close to zero due to the symmetry of the coils and currents. Therefore the expression of the force calculation was simplified .With the Eq. (21) of the force, the current needed in order to generate a force in a specified direction was found by solving the system displayed in Eq. (22). The system was solved using Maple and the result obtained is displayed in Eq. (23)(where $\varphi_U(\theta)$, $\varphi_V(\theta)$ and $\varphi_W(\theta)$ are the flux generated by the magnets in each phase and where the expression of the parameter κ are both given in the annexes below. Those equations were then implemented in the control system of the BELM in order to estimate the forces and choose the currents needed in order to get a specific force.

$$\frac{\partial W}{\partial x_o} = f_{x_o} = [I]^t \wedge \left[\frac{\partial \varphi_{mag}}{\partial x_o}\right] \tag{21}$$

$$\begin{cases} f_{x_o} = [I]^t \wedge \left[\dfrac{\partial \varphi_{mag}}{\partial x_o}\right] \\ f_{y_o} = [I]^t \wedge \left[\dfrac{\partial \varphi_{mag}}{\partial y_o}\right] \\ i_{Us} + i_{Vs} + i_{Ws} \end{cases} \tag{22}$$

$$\begin{cases} i_{Us} = -\dfrac{\left(\dfrac{\partial \varphi_V(\theta)}{\partial x_o} - \dfrac{\partial \varphi_W(\theta)}{\partial x_o}\right) f_{y_o} + \left(\dfrac{\partial \varphi_V(\theta)}{\partial y_o} - \dfrac{\partial \varphi_W(\theta)}{\partial y_o}\right) f_{x_o}}{2 \cdot \kappa} \\ i_{Vs} = \dfrac{\left(\dfrac{\partial \varphi_U(\theta)}{\partial x_o} - \dfrac{\partial \varphi_W(\theta)}{\partial x_o}\right) f_{y_o} + \left(\dfrac{\partial \varphi_U(\theta)}{\partial y_o} - \dfrac{\partial \varphi_W(\theta)}{\partial y_o}\right) f_{x_o}}{2 \cdot \kappa} \\ {}_{Vs} = -\dfrac{\left(\dfrac{\partial \varphi_U(\theta)}{\partial x_o} - \dfrac{\partial \varphi_V(\theta)}{\partial x_o}\right) f_{y_o} + \left(\dfrac{\partial \varphi_U(\theta)}{\partial y_o} - \dfrac{\partial \varphi_V(\theta)}{\partial y_o}\right) f_{x_o}}{2 \cdot \kappa} \end{cases} \tag{23}$$

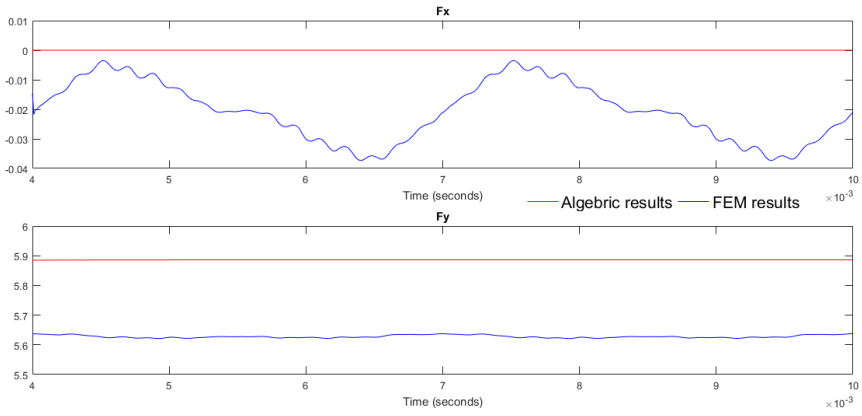

Fig. 4 Comparison of the force generation results between the algebraic calculation and the FEM results

4. Control of the bearingless machine

Using the model defined in section 2, the different equations for the voltage Eq. (6) Eq. (7) have been transferred to the frequencies domain (s domain). The obtained equations in Eq. (25) Eq. (26) are used as the base for the control of the machine. To start the control of the torque the current responsible for the torque is transformed into a dq axis. Through knowing that the torque is the product of current in the q axis and the flux created by the permanent magnets, the value for the current can be easily defined as shown below Eq. (27). The whole the system is set with a PI for each function. The corrector's parameters have been chosen via pole placement to obtain a second order system with a damping of 0.7 and have a response time of 100µs. The stability of the controller is then investigated, to do so the phase and gain margin of the controllers are calculated. In both cases the Gain margin is infinite, whilst for the suspension controller the phase margin is 76.4 deg and for the torque controller 62.5 deg. Those large margins should guarantee the stability of our system, but the closed loop system now has zeros generated by the corrector. The zeros don't affect the final values of our system but might affect the transient and therefore might generate some unexpected behavior of the system. To solve this, a bloc T(s) is added in order to cancel the zeros. In order to take into account the power electronics in the system, a bloc simulating an inverter has been added to the system. The system then has a bandwidth of 30kHz, as shown in the bode diagram of the close loop transfer function of the system **Error! Reference source not found.**.To take into account the presence of the power electronics, the system also includes saturation of the voltage V_s° as the DC link of a driver is fixed. To avoid problems resulting from the control saturating the inverter, a back calculation anti-windup is added to the system. The shaft of the BELM is modeled as a Jeffcott rotor with eccentricity. The displacement of the rotor without any action of the BEM is compared to displacement where the BELM is active. With the initial vibration of 1µm, which is the maximum tolerated by the seal, the vibration is reduced to 0.2µm, as shown on the Fig. 8 where a reduction of the vibration of about 80% was be observed..

$$\underline{V_{Us}} = 2 \cdot R \cdot \underline{I_{Us}} + 2 \cdot L_s \cdot s \cdot \underline{I_{Us}} \tag{25}$$

$$\underline{V_{Um}} = \frac{1}{2} \cdot \left(R \cdot \underline{I_{Um}} + L_m \cdot s \cdot \underline{I_{Um}} + \underline{V_{Us}} \right) + \underline{E_U} \tag{26}$$

$$i_{mq} = \frac{Torque}{\varphi_{mag}} \quad i_{md} = 0 \tag{27}$$

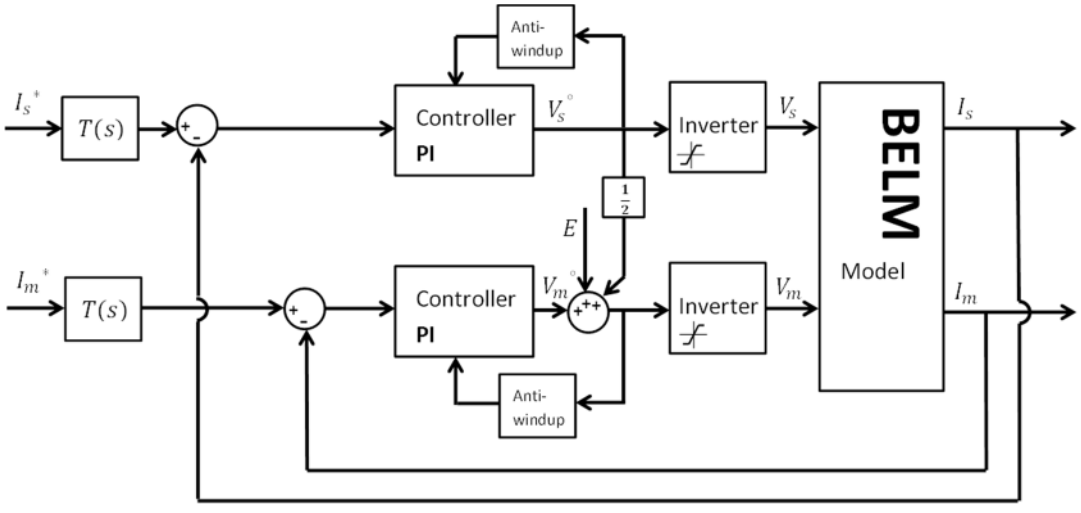

Fig. 5 Schematic of the control system's structure

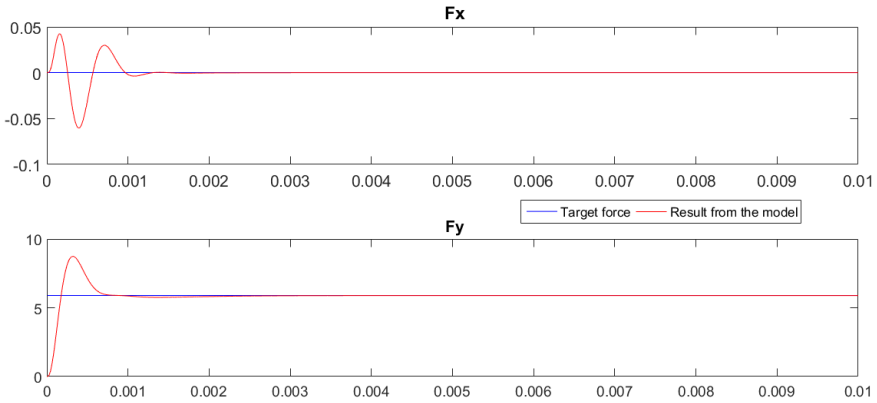

Fig. 7 Regulation of the force

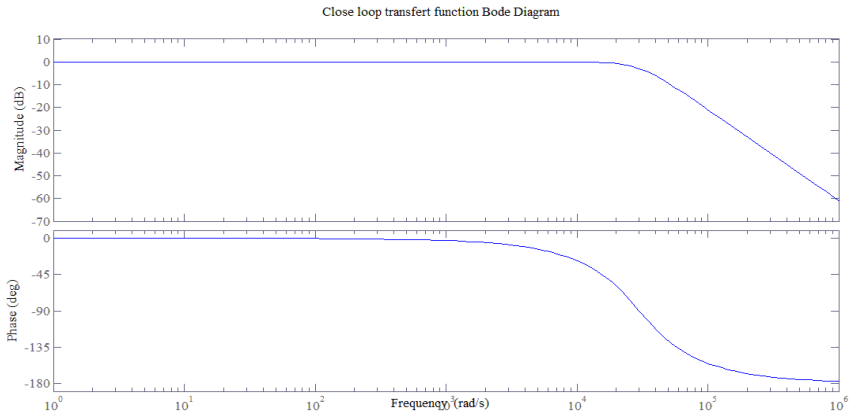

Fig. 6 Bode diagram of the close loop system

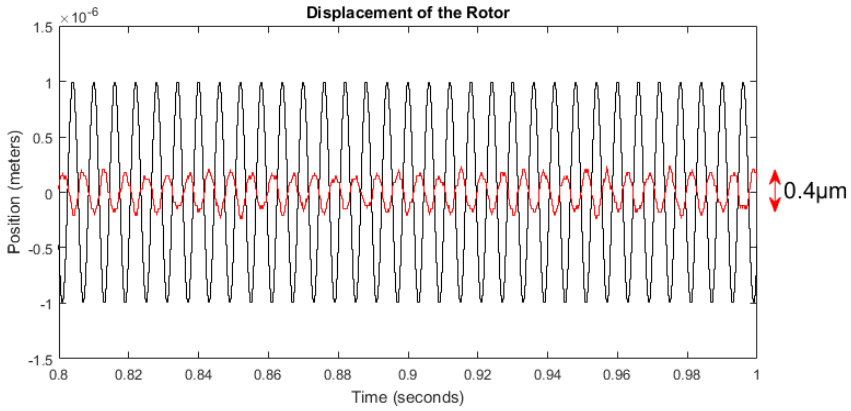

Fig. 8 Reduction of the vibration using the bearingless capabilities of the machine.

5. Conclusion

This paper demonstrated and detailed the control of a single winding bearing-less machine. By separating the control of the suspension and the torque, two parameters L_s and L_m were introduced to simplify the definition of the electrical equations of the BELM. The energy from forces generated by the BELM was calculated with an algebraic equation with a difference of 5% compared to the FEM simulation. A control system for the BELM was then designed to obtain a response time of 100 µs and a damping a factor of 0.7. The controller was designed to stay robust to perturbation and variations, therefore the different margins of the controllers were monitored in order to stay in an acceptable range. To take in account the presence of the power electronics, an anti-windup was implemented in order to limit the saturation on the inverter. The system was then then able to reduce the vibration on a Jefcott rotor by about 80% for the air riding seal. The next step would be to incorporate a more accurate model of the shaft in order to visualize how the BELM could act upon the displacement of the shaft when the seal is set far from the BELM.

6. Annexes

$$\lim_{\substack{x_o \to 0 \\ y_o \to 0}} \frac{\left(\cos(\beta)^2 - 1\right) \cdot x_o + \sin(\beta) \cdot \cos(\beta) \cdot y_o}{\sqrt{\cos(\beta)^2 \cdot \left(x_o^{\,2} - y_o^{\,2}\right) + 2 \cdot \sin(\beta) \cdot \cos(\beta) \cdot x_o \cdot y_o - x_o^{\,2} + R_{rotor}^{\,2}}} = 0 \tag{17}$$

$$\kappa = \frac{\partial \varphi_U(\theta)}{\partial x_o} \cdot \left(\frac{\partial \varphi_V(\theta)}{\partial y_o} - \frac{\partial \varphi_W(\theta)}{\partial y_o} \right) + \frac{\partial \varphi_V(\theta)}{\partial x_o} \cdot \left(\frac{\partial \varphi_U(\theta)}{\partial y_o} - \frac{\partial \varphi_W(\theta)}{\partial y_o} \right) + \frac{\partial \varphi_W(\theta)}{\partial x_o} \cdot \left(\frac{\partial \varphi_U(\theta)}{\partial y_o} - \frac{\partial \varphi_V(\theta)}{\partial y_o} \right) \tag{23}$$

[1] **A. Chiba, T. Fukao, and M. Azizur Rahman, "Vibration Suppression of a Flexible Shaft With a Simplified Bearingless Induction Motor Drive," *Industry Applications, IEEE Transactions on,* vol. 44, pp. 745-752, 2008.**

[2] **C. Liu, Y. Yang, and Z. Deng, "Vibration control strategy for bearingless switched reluctance motors," in *Electrical Machines and Systems (ICEMS), 2014 17th International Conference on*, 2014, pp. 1675-1680.**

[3] **Y. Iiyama, K. Soutome, and A. Chiba, "A novel middle-point current-injection type bearingless motor for vibration suppression," in *Energy Conversion Congress and Exposition (ECCE), 2010 IEEE*, 2010, pp. 1693-1698.**

[4] **Y. Uemura, Nakahata, T. ,Chiba, A., "Vibration Suppression of A Middle-Point Current-Injection Type Bearingless Motor at 50000r/min," in *ISMB14*, ed. http://www.magneticbearings.org/, 2014.**

[5] **R. Oishi, S. Horima, H. Sugimoto, and A. Chiba, "A Novel Parallel Motor Winding Structure for Bearingless Motors," *Magnetics, IEEE Transactions on,* vol. 49, pp. 2287-2290, 2013.**

[6] **A. Chiba, S. Horima, and H. Sugimoto, "A principle and test results of a novel bearingless motor with motor parallel winding structure," in *Energy Conversion Congress and Exposition (ECCE), 2013 IEEE*, 2013, pp. 2474-2479.**

[7] **B. Lapotre, Takorabet, N., Tabar, F.M., Lateb, R. and Silva, J.D., "Radial Force Modeling of bearingless Motors Based on, Spectral Analysis of Field Sources," presented at the ISMB14, Linz, 2014.**

[8] **B. Wenshao, H. Shenghua, W. Shanming, and W. Fang, "A Kind of Generalized Analytical Model on Magnetic Suspension Force of Bearingless Motor and its Application," in *Industrial Electronics and Applications, 2007. ICIEA 2007. 2nd IEEE Conference on*, 2007, pp. 1663-1668.**

[9] **A. Chiba, M. A. Rahman, and T. Fukao, "Radial force in a bearingless reluctance motor," *Magnetics, IEEE Transactions on,* vol. 27, pp. 786-790, 1991.**

[10] **Akira Chiba, Tadashi Fukao, Osamu Ichikawa, Masahide Oshima, Masatsugu Takemoto, and D. G. Dorrell, *Magnetic Bearings and Bearingless Drives*: Newes, 2005.**

7. Acknowledgement

The research leading to these results has received funding from the People Programme (Marie Curie Actions) of the European Union's Seventh Framework Programme (FP7/2007-2013) under REA grant agreement no 608322.

The help and support of Ramdane LATEB and Joaquim DA SILVA from SKF Magnetic Mechatronics, who allowed me to stay at SKF Magnetic Mechatronics for 6 months.